

# Predictive Cruise Control: Utilizing Upcoming Traffic Signal Information for Improving Fuel Economy and Reducing Trip Time

Behrang Asadi and Ardalan Vahidi

**Abstract**—This brief proposes the use of upcoming traffic signal information within the vehicle’s adaptive cruise control system to reduce idle time at stop lights and fuel consumption. To achieve this goal an optimization-based control algorithm is formulated that uses short range radar and traffic signal information predictively to schedule an optimum velocity trajectory for the vehicle. The control objectives are: timely arrival at green light with minimal use of braking, maintaining safe distance between vehicles, and cruising at or near set speed. Three example simulation case studies are presented to demonstrate the potential impact on fuel economy, emission levels, and trip time.

**Index Terms**—Fuel economy, model predictive control (MPC), predictive cruise control (PCC), traffic light preview.

## I. INTRODUCTION

AMERICAN drivers spend a total of 40 h per year idling in traffic. The cost of fuel used during this idle time is 78 billion dollars per year [1]. A big portion of our idle time is the time spent behind traffic lights. Poor traffic signal timing is believed to account for an estimated 10% of all traffic delays on major roadways (about 300 million vehicle hours) [2]. Effective advanced traffic signal control methods such as traffic-actuated signals and signal synchronization have been deployed at many traffic intersections which help us save precious time and expensive fuel every day. Such measures, however, are very costly to implement and maintain; just the annual cost of signal timing updates is estimated at 217 million dollars a year according to [3]. Even with these measures in place, we often cruise at full speed toward a green and have to come to a sudden halt when the light turns red. This lack of information about the “future” state of the traffic signal increases fuel consumption, trip time, and engine and brake wear. In an ideal situation, if the future of a light timing and phasing are known, the speed could be adjusted for a timely arrival at green.

While maybe unrealistic a few years ago, communicating traffic signal state to the vehicles in advance is not far-fetched today. In Europe some lights are capable of two-way communication with public transportation vehicles [4]. In the U.S., researchers are now experimenting with broadcasting red light warnings to vehicles to improve traffic intersection safety [5], [6]. The INTERSAFE project in Europe is another example of light to vehicle communication for improved intersection safety



Fig. 1. Schematic of telematics-based PCC.

[7]. As demonstrated in [6], the required information broadcast technology is available today and is expected to be more widely deployed in the near future.

This brief focuses on employing upcoming light time and phase information within the vehicle’s adaptive cruise control system to reduce: 1) wait time at stop lights and 2) fuel consumption, which may also reduce total trip time and CO<sub>2</sub> emissions. To achieve this goal an optimization-based control algorithm will be formulated for each equipped vehicle that uses short range radar and traffic signal timing information to schedule an optimum velocity trajectory. The objectives are timely arrival at green light with minimal use of braking, maintaining safe distance between vehicles, and cruising at or near set speed. Fig. 1 shows a schematic of this proposed concept.

Adaptive cruise control is now in production and a well-matured technology. Many ideas on intelligent transportation system (ITS) have been explored extensively during the 1990’s within intelligent highway initiatives in the U.S., Japan, and Europe [8]. Optimal traffic management at intersections has been mainly studied from a signal-timing optimization perspective (signal synchronization) [9]–[11]. More recently and for futuristic autonomous vehicles, Dresner *et al.* [12], [13] have proposed replacing traffic lights and stop signs by intelligent lights: via a two way communication protocol, the autonomous vehicles call the intersection ahead to reserve a time-space slot to pass; which among other things can help improve the fuel economy. Also in the late 1990’s and within the Urban Drive Control project use of traffic signal information for improving traffic flow was studied in Italy [14]. Voluntary use of future signal and traffic information has recently regained momentum under Cooperative Intersection Collision Avoidance Systems (CICAS) initiative mainly for improving intersection safety [15], [16].

The predictive cruise control (PCC) concept proposed in this brief utilizes the adaptive cruise control function in a predictive manner to simultaneously improve fuel economy and reduce signal wait time. The proposed predictive speed control mode differs from current adaptive cruise control systems in that besides maintaining a safe gap between vehicles, it: 1) decreases use of brakes, thus reducing brake wear and kinetic energy loss; 2) is applicable in stop and go traffic; and more importantly 3)

Manuscript received June 02, 2009; revised January 14, 2010; accepted March 24, 2010. Manuscript received in final form April 02, 2010. Recommended by Associate Editor S. Liu.

The authors are with the Department of Mechanical Engineering, Clemson University, Clemson, SC 29634 USA (e-mail: basadi@clemson.edu; avahidi@clemson.edu).

Color versions of one or more of the figures in this brief are available online at <http://ieeexplore.ieee.org>.

Digital Object Identifier 10.1109/TCST.2010.2047860

receives a timing signal from an upcoming traffic light in advance to safely and smoothly speed up or down to a timely arrival at green light whenever possible, therefore reducing idling at red.

These sometimes conflicting objectives are unified under an optimization-based model predictive control (MPC) framework. The proposed MPC formulation allows tracking a target speed, calculated based on traffic signal information, while reducing brake use. At the same time it enforces several physical constraints including a safe distance to the vehicle in front. Simulation of complex stop and go situations is facilitated relying on MPC as the “driving brain” of each vehicle. Because model predictive control is an optimization-based approach, it may handle the traffic imposed constraints more systematically than the existing microscopic and macroscopic models for traffic simulation [17]–[19]. Many underlying functions or rules required to determine procession of vehicles limit our ability to embed systematic optimization routines in the existing methods.

Section II formulates the methodology for planning a desired velocity profile around red lights and the tracking of this target velocity under motion constraints using model predictive control. Section II-C describes a detailed powertrain model used for evaluating the fuel economy and CO<sub>2</sub> emissions of the vehicle. Three simulation case studies are presented in Section III to illustrate application of the proposed methodology in single- and multi-vehicle scenarios. Conclusions are presented in Section IV.

## II. METHODOLOGY

The objective is to find the optimal vehicle velocity that reduces idling at red lights given the future state of traffic lights. One of the analytical challenges unique to this optimal control problem is the dynamic switching of lights to red and green. These types of motion constraints render the feasible solution space non-convex. Solution of a non-convex optimization problem is computationally intensive and may not converge to the global optimum. In order to find a near-optimal solution with reasonable level of computations, we handle the problem at two levels: 1) a set of logical rules that calculates a reference velocity for timely arrival at green lights combined with 2) a model predictive controller that tracks this target velocity. The resulting solution may be sub-optimal but can be implemented in real-time. A simple model of the vehicle will be used at the supervisory level for velocity planning; but the fuel economy, CO<sub>2</sub> emissions, and drivability will be later evaluated using a detailed model of the powertrain.

### A. Reference Velocity Planning

A reference velocity  $v_{\text{target}}$  is determined based on the driver set cruise speed and also the signal received from the upcoming traffic light. The basic idea is to safely: 1) increase  $v_{\text{target}}$ , up to a maximum allowable, when there is enough green time to pass or otherwise 2) decrease  $v_{\text{target}}$ , down to a minimum allowable, to arrive at the next green. All will be done considering driver’s set cruise control speed. The objective is to avoid stopping at a red light if feasible.

It is assumed that the approximate distance to the next traffic light(s) is known at each time and shown by  $d_i$ . The subscript  $i$

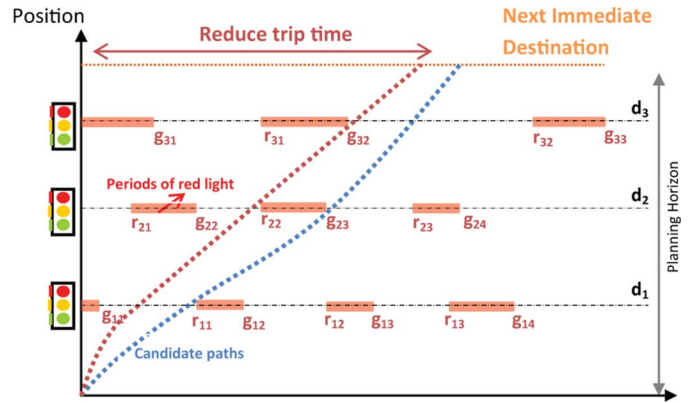


Fig. 2. Schematics map of red lights distributed over space-time. The graphics shows how a PCC car passes two consecutive traffic intersection without having to stop at a red.

denotes the light number in a sequence of traffic lights, i.e.,  $d_1$  is the approximate distance to the first upcoming light and  $d_2$  to the second light at each time. The light(s) update and broadcast their expected sequence of green and red times regularly. Suppose  $g_{ij}$  is start of the  $j$ th green of the  $i$ th traffic light and  $r_{ij}$  is start of the  $j$ th red of the  $i$ th light. For example, light number 1 broadcasts, at regular intervals, a sequence

$$[g_{11}, r_{11}, g_{12}, r_{12}, g_{13}, \dots] = [40, 100, 150, 200, 240, \dots]$$

which implies the first traffic light is currently red, it will turn green in 40 s, red in 100 s, green again in 150 s, and so forth. Fig. 2 shows a schematic of the map formed at each time step based on the information received from the lights. Equipped vehicles can use the remaining distance to the next light(s) and the green and red sequence to set their target speed. This target speed (slope of each path) should be in the feasible range  $[v_{\min}, v_{\max}]$ , where  $v_{\min}$  is the road’s minimum speed limit and  $v_{\max}$  is the smaller of two quantities: the velocity set by the driver and the road’s maximum speed limit. Other constraints, such as acceleration constraints, maintaining safe distance to the front vehicle, and reducing use of brakes are handled separately by a dynamic optimization scheme (details in Section II-B).

The following steps determine the target speed at each step  $k$ .

- 1) For a vehicle to pass during the first green of the first light, its velocity should be in the interval  $[d_1/r_{11}, d_1/g_{11}]$ . This is only feasible if this interval has a set intersection with the feasible speed interval of  $[v_{\min}, v_{\max}]$ . If this set intersection is empty, passing through the first green without stopping at red is deemed infeasible. In that event, feasibility of passing during the next green interval is checked and the process is repeated until for some  $i$ th interval  $[d_1/r_{1i}, d_1/g_{1i}]$  has a set intersection with  $[v_{\min}, v_{\max}]$ . This set intersection is mathematically characterized by

$$\left[ \frac{d_1}{r_{1i}}, \frac{d_1}{g_{1i}} \right] \cap [v_{\min}, v_{\max}] \quad (1)$$

and determines the range of speed that ensures passing the first light without having to stop at a red.

For example assume the speed limits are  $[v_{\min}, v_{\max}] = [5, 20]$  m/s and the distance to the first traffic light is 1000 m. The first light broadcasts

$$g_{11} = 5 \text{ s}, \quad r_{11} = 25 \text{ s}, \quad g_{12} = 40 \text{ s}, \quad r_{12} = 100 \text{ s}$$

then

$$\left[ \frac{d_1}{r_{11}}, \frac{d_1}{g_{11}} \right] = [40, 200] \text{ m/s}$$

does not meet the speed limit. The second interval

$$\left[ \frac{d_1}{r_{12}}, \frac{d_1}{g_{12}} \right] = [10, 25] \text{ m/s}$$

intersects with the feasible speed at  $[10, 20]$  m/s. Therefore, if the velocity of the vehicle is chosen between 10 and 20 m/s, the vehicle passes the first light without having to stop. If no feasible set intersection is found, stopping at the light will be unavoidable and no further check is necessary.

- 2) If passing without stop at the first light is determined to be feasible, the process in step 1 is repeated for the second traffic light by checking the set intersections

$$\left[ \frac{d_2}{r_{2i}}, \frac{d_2}{g_{2i}} \right] \cap [v_{\min}, v_{\max}]$$

and picking the first non-empty one.

- 3) Next, the set intersection of the feasible range of speeds determined in step 1 and that of step 2 is calculated. A non-empty solution  $[v_{\text{low}}, v_{\text{high}}]$  indicates feasibility of passing the two lights without having to stop at a red by maintaining a constant speed. However an empty solution does not imply that stopping at red is necessarily required. It only means that passing the two consecutive lights with the same speed is not feasible. In that event, the vehicle can readjust its target speed after passing the first light to pass the green of the second light.
- 4) The process is continued by checking the next lights until a stop at red becomes unavoidable. The last feasible range  $[v_{\text{low}}, v_{\text{high}}]$  is an appropriate target velocity. In this brief we set  $v_{\text{target}} = v_{\text{high}}$  for reducing trip time.<sup>1</sup>

Note that the target velocity is updated at each sampling time and therefore may change at each instant based on vehicle's position and the most recent information from the lights. This set of rules is not necessarily "optimal", but helps break down a fundamentally non-convex optimization problem to a simpler real-time implementable one. Tracking this target velocity, maintaining a safe distance to the front vehicle, and reducing

<sup>1</sup>One can argue that in some scenarios a decreasing target velocity profile may require less fuel than a constant target velocity with same travel time. One can check, for example, feasibility of a target velocity decreasing linearly where the constant deceleration rate  $a$  before a light can be found from the following kinematic equation:

$$d_1 = \frac{1}{2} a g_{11}^2 + v_0 g_{11}$$

where  $v_0$  is the initial speed. Because searching for variable speed profiles increases the search space and the computational time, such profiles are not considered in this brief.

use of brakes are handled by the optimization scheme which is described next.

### B. Optimal Tracking of the Reference Velocity

A simple model of the vehicle is used at the supervisory level for calculating the vehicle acceleration based on effective traction force of the engine  $f_{\text{engine}}$  or braking force  $f_{\text{brake}}$  and the road forces  $f_d$ . For the  $i$ th vehicle with mass  $m_i$ , the longitudinal dynamics is [20]

$$m_i \frac{d^2 x_i}{dt^2} = f_{\text{engine}}^i - f_{\text{brake}}^i + f_d^i \quad (2)$$

where  $f_d^i$  lumps the road forces including aerodynamic drag, rolling resistance, and road grade forces

$$f_d^i = -c_D v_i^2 - m_i g (\sin(\theta) + \mu \cos(\theta)) \quad (3)$$

where  $\theta$  is the road grade,  $c_D$  is a "lumped" drag coefficient,  $\mu$  is the coefficient of rolling resistance, and  $g$  is gravitational acceleration. The  $f_d^i$  term is treated as a measured disturbance and updated at each sample time. Equation (2) can be written in the following state-space discretized form

$$\begin{aligned} z_i(k+1) &= A z_i(k) + B_u u_i(k) + B_w w_i(k) \\ y_i(k) &= C z_i(k) \end{aligned} \quad (4)$$

where  $z_i = [x_i \quad v_i]^T$  is the state vector,  $u_i = [f_{\text{engine}}^i \quad f_{\text{brake}}^i]^T$  is the control input, and  $w_i = [f_d^i]$  is the measured disturbance. The main outputs of interest are  $y_i = [x_i \quad v_i]^T$ ; however other outputs are introduced in the simulation code to handle the gap inequality constraint described later. The matrices  $A \in \mathbb{R}^{2 \times 2}$ ,  $B_u \in \mathbb{R}^{2 \times 2}$ ,  $B_w \in \mathbb{R}^{2 \times 1}$ , and  $C \in \mathbb{R}^{2 \times 2}$  are the discretized system matrices. The engine and brake forces are manipulated for tracking the target speed as closely as possible while maintaining a safe distance to the front vehicle. These objectives along with the desire to reduce use of service brakes can be unified in a model predictive control (MPC) framework. The control performance index at each step  $k$  for the  $i$ th vehicle is defined as

$$J_i(k) = \sum_{j=k}^{k+P-1} [w_1 (v_i(j) - v_{\text{target}}(j))^2 + w_2 (f_{\text{brake}}^i(j))^2]. \quad (5)$$

The trip time is reduced by setting  $v_{\text{target}}$  equal to maximum feasible speed as explained in the previous section. This constant-velocity solution may be suboptimal; the truly optimal solution requires explicit optimization of trip time over space of all functions  $v_i$ .

Here  $w_1$  and  $w_2$  are simply penalty weights for each term. The above index penalizes deviations of vehicle speed  $v_i$  from the target speed  $v_{\text{target}}$  and also reduces use of brake force over a future prediction window of  $P$  steps. Reduced use of service brakes in the cost function indirectly contributes to fuel savings. Fuel consumption is not explicitly penalized; this allows use of the simpler vehicle model for control design. Fuel savings will be later evaluated using a detailed model of the vehicle's powertrain.

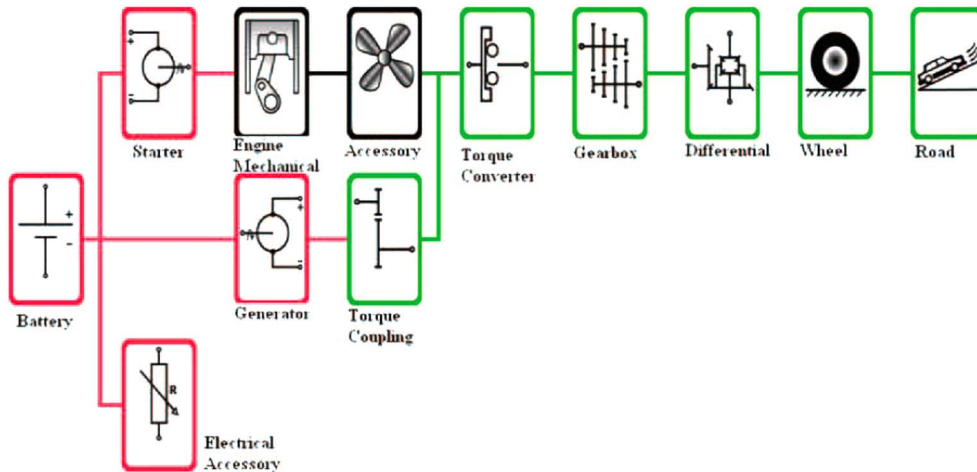


Fig. 3. Schematic of a PSAT powertrain model.

The speed limit, engine and brake force limits, and the minimum safe following distance are imposed as pointwise-in-time inequality constraints. The constraints should be satisfied over the future prediction horizon  $\forall j \in \{k, k+1, \dots, k+P-1\}$ . The speed limit constraint is

$$v_{\min} \leq v_i(j) \leq v_{\max} \quad (6)$$

where  $v_{\min}$  and  $v_{\max}$  are speed limits and should also be smaller than the driver set speed. Bounds on the traction force are represented by

$$\begin{aligned} 0 &\leq f_{\text{engine}}^i(j) \leq f_{\text{acceleration}}^{\max} \\ 0 &\leq f_{\text{brake}}^i(j) \leq f_{\text{deceleration}}^{\max} \end{aligned} \quad (7)$$

where  $f_{\text{acceleration}}^{\max}$  and  $f_{\text{deceleration}}^{\max}$  depend on tire and road condition and also maximum engine and braking torque capability. The minimum safe distance between the vehicle  $i$  and the front vehicle (target) should be a function of the vehicle speed and is chosen as [8]

$$x_{\text{target}}(j) - x_i(j) \geq \alpha v_i(j) + \beta \quad (8)$$

where  $\beta$  is a “static gap” parameter and determines the minimum gap needed when the vehicles are stopped and  $\alpha$  is a “dynamic gap” parameter providing extra gap with increased speed. Note that when the vehicle is approaching a red light, the light is considered similar to a stopped vehicle and the position  $x_{\text{target}}$  is fixed to the position of the light. This ensures that the vehicle comes to a stop with distance  $\beta$  from the light ( $x_{\text{target}} \geq x_i + \beta$ ).

The cost function (5) subject to the model equation (4) and inequality constraints (6), (7), and (8) is minimized at each sample time to determine the sequence of next  $N \leq P$  control inputs  $U_i(k) = [u_i(k) \ u_i(k+1) \ \dots \ u_i(k+N-1)]$  over the future horizon  $P$ . When  $N < P$  the remaining control moves  $[u_i(k+N) \ u_i(k+N+1) \ \dots \ u_i(k+P-1)]$  are assumed to be zero. According to the standard MPC design, only the first entry of the control sequence  $U_i(k)$ , is applied to the vehicle; the optimization horizon is moved one step forward, the model and constraints are updated if necessary, and the optimization

process is repeated to obtain the next optimal control sequence  $U_i(k+1)$  [21]–[23].

### C. Evaluation of Fuel Savings Potential With a Detailed Powertrain Model

The MPC solution generates a constraint-admissible velocity profile that follows the set target speed as closely as possible. In order to estimate the fuel economy of the vehicle when following this optimal velocity trajectory, a production vehicle is selected and its powertrain model is assembled from the extensive database of Powertrain System Analysis Toolkit (PSAT). PSAT, developed by Argonne National Laboratory [24], is a powerful simulation tool for evaluating the fuel economy of conventional and hybrid vehicles when following a prescribed velocity cycle. Its physics-based component models combined with empirical maps obtained from production vehicles allow high-fidelity evaluation of fuel economy. Fig. 3 shows schematics of a PSAT powertrain model. This is a conventional (non-hybrid) powertrain with an automatic transmission. The models for torque converter, transmission, and vehicle dynamics are all very detailed and include several dynamic states and switching modes. Details such as electrical accessory loads, the starter, generator, etc. are not overlooked, and are modeled for simulation accuracy.

PSAT is a “forward-looking” causal simulation tool in which the vehicle speed is determined by the combined influence of road loads and engine (or brake) torque at the wheels. The resulting velocity is compared to the prescribed desired velocity; the difference is fed to a driver model (a PI controller) which in turn determines a torque demand. The torque demand is met by the engine (or brake) torques and the above simulation loop is repeated. The engine fuel rate is determined using an empirical engine map and as a function of engine speed and engine torque. The fuel rate is integrated over the whole cycle time to determine the amount of fuel used.

## III. SIMULATION CASE STUDIES

This section presents the results of a few simulations performed to demonstrate validity of the proposed PCC methodology and to observe the fuel economy, emissions, and travel

TABLE I  
MPC PARAMETERS

| parameter                | description           | value | units (SI)          |
|--------------------------|-----------------------|-------|---------------------|
| $T_s$                    | sample time           | 0.2   | s                   |
| $P$                      | prediction horizon    | 8     | s                   |
| $N$                      | control horizon       | 2     | s                   |
| $W_1$                    | penalty weight 1      | 3000  | (m/s) <sup>-2</sup> |
| $W_2$                    | penalty weight 2      | 150   | N <sup>-2</sup>     |
| $\alpha$                 | dynamic gap parameter | 0.2   | s                   |
| $\beta$                  | static gap parameter  | 5     | m                   |
| $f_{acceleration}^{max}$ | max positive traction | 3000  | N                   |
| $f_{deceleration}^{max}$ | max negative traction | 6800  | N                   |

time gains in these example simulations. To understand the impact of PCC on the average and under different traffic lights and vehicle parameters, an extensive simulation study is needed which is outside the scope of the current brief. We hope the following simulation results motivate a detailed statistical analysis in the future.

The simulations are run first with the PCC off which serves as a baseline for comparison and then with PCC on during which advanced information of the lights phasing and timing is available. The comparison baseline is a vehicle without advanced access to signal phasing and timing information. For a fair comparison, the baseline vehicle is assumed to operate in adaptive cruise control mode as well.<sup>2</sup> The baseline vehicle tracks a target velocity using the MPC strategy explained in Section II-B. Its controller minimizes (5) subject to the same model equation (4) and inequality constraints (6)–(8). However the target velocity  $v_{target}$  is always equal to the driver set speed for the baseline vehicle. The need for a timely stop at red light is enforced through the constraint (8) and by fixing  $x_{i+1}$  to the position of the light as soon as the light turns amber or if an upcoming light is found to be red (thus no advanced phase and time information).

The parameters of the supervisory level controller are summarized in Table I. In all simulations, the vehicle mass is assumed to be  $m = 1000$  kg. Maximum acceleration is assumed to be  $a_{max} = 3$  m/s<sup>2</sup> which is a conservative estimate of the maximum acceleration capability of a midsize vehicle. From there we calculate  $f_{acceleration}^{max} = ma_{max} = 3000$  N. Assuming braking on dry asphalt, the coefficient of braking is chosen to be  $\mu_b = 0.69$  [20]. The maximum possible braking force is then calculated as  $f_{deceleration}^{max} = \mu_b mg \approx 6800$  N. The sampling time of 0.2 s allowed capturing the relevant dynamics. After several trials, prediction and control horizons of 8 and 2 s, respectively, were found to be adequate and beyond this the performance did not change considerably. The penalty weights  $W_1$  and  $W_2$  were tuned to track the target velocity with reasonable braking effort. The gap parameters are most relevant in multi-vehicle simulations and are chosen to ensure sufficient distance between vehicles.

<sup>2</sup>Adaptive cruise control assumption can be thought of as a systematic mean to model a driver behavior in flowing traffic. In other words the comparison is not limited only to ACC equipped vehicles.

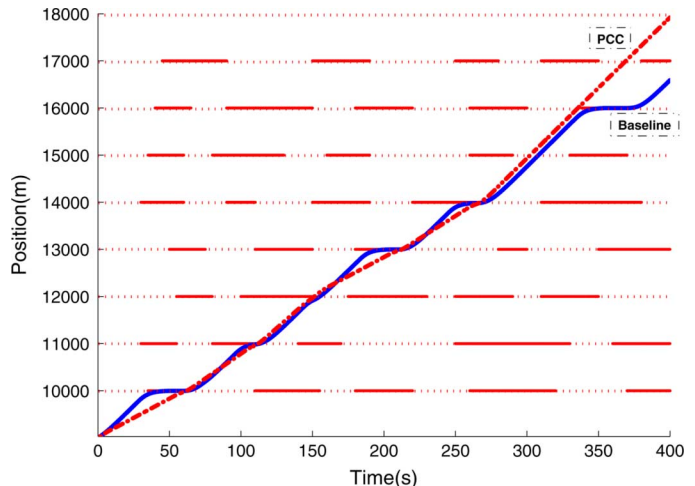


Fig. 4. Trajectory of PCC and baseline vehicles with respect to the red-light map. Horizontal solid lines represent red intervals.

### A. Single Vehicle Scenario

1) *Case I-Suburban Driving*: The first simulation case study is created to approximate suburban driving conditions: the driver set speed is 30 m/s, the maximum speed is  $v_{max} = 30$  m/s, and the minimum speed  $v_{min}$  is zero. A sequence of 10 traffic lights spaced at 1 km intervals is assumed for this simulation study. The light timing and phasing is assumed to be fixed and independent of the incoming traffic. Future work can consider situations of synchronized or traffic-actuated lights. Fig. 4 summarizes the light timing information. Also on this graph we show the trajectory of PCC and baseline vehicles.

Fig. 5 shows the velocity profile, control inputs, and the distance traveled by the baseline vehicle. Zero portions of the velocity profile show that the baseline vehicle stops at multiple red signals. In a period of 400 s, the vehicle travels the distance of 7.66 km and passes 7 lights. The average velocity is therefore 19.15 m/s. During the same time and with the same initial conditions the PCC-equipped vehicle was able to travel 8.92 km as shown in Fig. 6. By predictive use of signal information, the PCC vehicle schedules its velocity to a timely arrival at a green light whenever possible. As a result the average velocity is 22.32 m/s which is a 16.5% improvement over the baseline vehicle. During the simulation the minimum and maximum speed constraints as well as all other constraints are met.

To evaluate the resulting fuel economy and emissions, an economy-sized passenger vehicle with the mass of 1000 kg and 5-speed automatic transmission was selected in PSAT. The vehicle has a 1.7 L 4-cylinder gasoline engine with the maximum power of 115 hp. The detailed vehicle model is assembled in PSAT v6.2. The velocity profiles shown in the first subplot of Figs. 5 and 6 are fed as inputs to the PSAT simulation environment. A driver-model follows this input velocities very closely. Table II summarizes the statistics of the resulting velocity and acceleration. The maximum acceleration and deceleration for both PCC and baseline vehicles are within

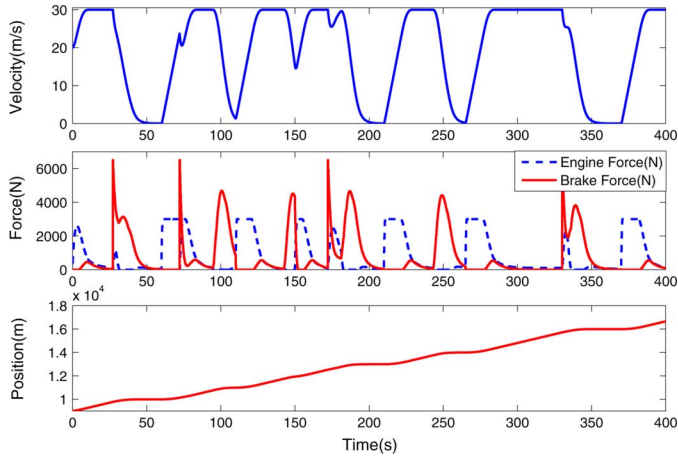


Fig. 5. Velocity, control inputs, and the position for a vehicle without advanced signal information.

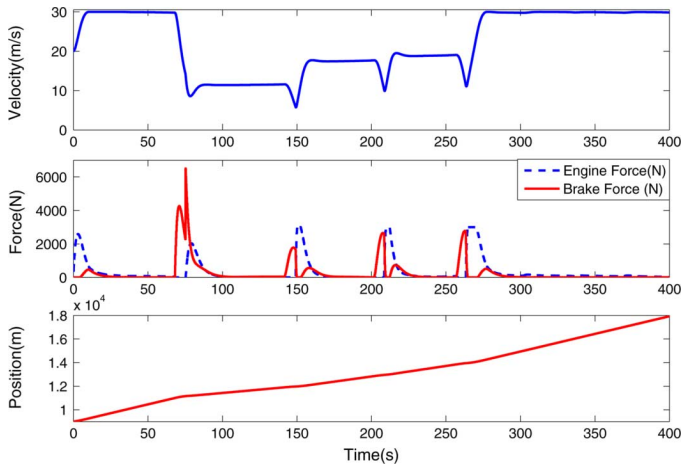


Fig. 6. Velocity, control inputs, and the position for a vehicle with advanced signal information.

TABLE II  
DRIVE-CYCLE STATISTICS FOR PCC AND BASELINE VEHICLES

| PCC vehicle      | Max   | Average | Standard Dev. | Unit    |
|------------------|-------|---------|---------------|---------|
| Speed            | 30.00 | 22.32   | 7.81          | $m/s$   |
| Acceleration     | 2.04  | 0.28    | 0.58          | $m/s^2$ |
| Deceleration     | -3.23 | -0.21   | 0.57          | $m/s^2$ |
| Baseline vehicle | Max   | Average | Standard Dev. | Unit    |
| Speed            | 30.00 | 19.15   | 11.79         | $m/s$   |
| Acceleration     | 2.04  | 0.97    | 0.87          | $m/s^2$ |
| Deceleration     | -3.10 | -0.79   | 1.03          | $m/s^2$ |

physical constraints and comparable to maximum acceleration and deceleration levels in many standard city cycles.<sup>3</sup> The calculated fuel economy and CO<sub>2</sub> emissions are shown in Table III. In this particular simulation, the PCC-equipped vehicle uses 47% less fuel with 56% less CO<sub>2</sub> emissions than the vehicle with the conventional ACC for the same travel time. These benefits are seen even though the PCC vehicle travels a longer distance.

<sup>3</sup>For example US06 Supplemental Federal Test Procedure (SFTP) which has been developed to address the shortcomings with the FTP-75 test cycle in the representation of aggressive, high speed and/or high acceleration driving behavior, rapid speed fluctuations, and *driving behavior following startup* has a maximum acceleration of 3.75 m/s<sup>2</sup> and maximum deceleration of -3.08 m/s<sup>2</sup>.

TABLE III  
PSAT SIMULATION RESULTS FOR AN ECONOMY-SIZE VEHICLE

| Value                             | PCC   | Baseline |
|-----------------------------------|-------|----------|
| Fuel Economy (miles/gallon)       | 28.72 | 19.22    |
| CO <sub>2</sub> Emissions(g/mile) | 290   | 453      |

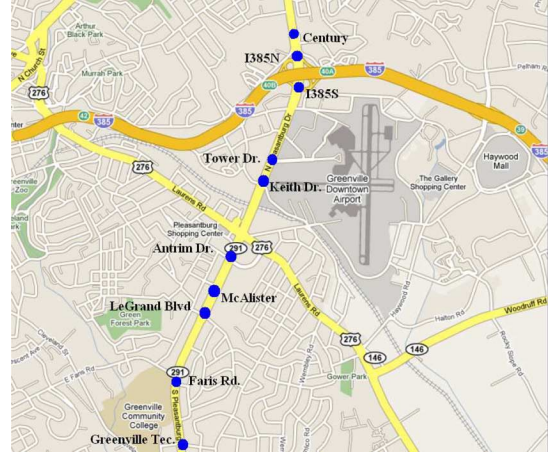


Fig. 7. Google map of a part of Pleasantburg Drive in Greenville, SC used in the second simulation case study.

To determine if real-time implementation of the proposed optimization-based strategy is computationally viable, we also recorded the total computational time for solving the MPC optimization problem. The simulations were run in SIMULINK on a dual-core Intel<sup>4</sup> Pentium IV processor with 1 GHz processing speed per core, 4 MB of cache, and 2 GB of RAM. An estimate of CPU time was obtained using the *CPU* command in MATLAB.<sup>5</sup> For a simulation interval of 400 s the CPU time for running the MPC optimization was 19.1 s.

2) *Case II-City Driving*: The second single vehicle simulation case study represents inner-city driving. For this we were able to acquire traffic signal phasing and timing data from a stretch of Pleasantburg Drive<sup>6</sup> inside the city of Greenville, SC. Fig. 7 shows a Google Map<sup>7</sup> of this street and 10 of its consecutive intersections selected for this study. The distances between these intersections have been measured using the map. Observing the posted speed limit of 45 m/h along Pleasantburg Drive, we set  $v_{\max} = 20$  m/s. The driver set speed is also selected at 20 m/s, and the minimum speed  $v_{\min}$  is set to zero. The other simulation parameters are those of Case I.

The simulations were run with two sets of initial conditions. Figs. 8 and 9 show the trajectories of PCC and baseline vehicles in these two scenarios. With the first set of initial conditions, the PCC vehicle saves 65 s of trip time with 29% less fuel (25.97 m/g versus 20.07 m/g for the baseline). If the start time is delayed by 20 s, the PCC's trip time advantage will only be 2 s

<sup>4</sup>Intel is a registered trademark of Intel Corporation, Santa Clara, CA.

<sup>5</sup>MATLAB and SIMULINK are registered trademarks of The MathWorks Inc. of Natick, MA.

<sup>6</sup>Pleasantburg Drive, south bound, starting from Century Drive and ending at Cleveland Street. The lights phasing and timing are those in place in April of 2009 and obtained from the Traffic Engineering Department of the City of Greenville.

<sup>7</sup>Google Map is a registered trademark of Google Inc., Mountainview, CA.

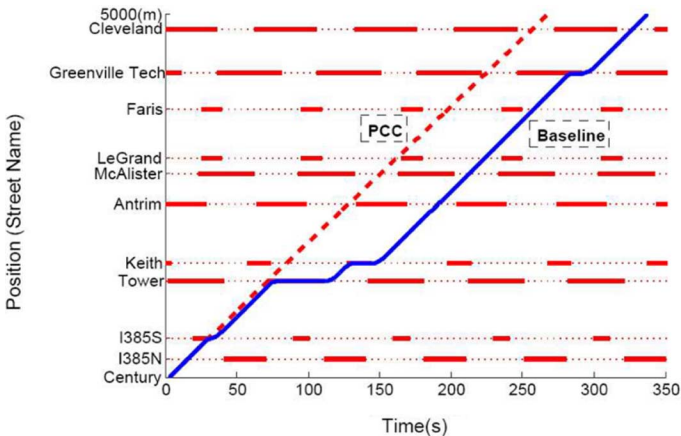


Fig. 8. First set of PCC and baseline trajectories simulated with Pleasantburg Drive signal timings. Horizontal solid lines represent red intervals.

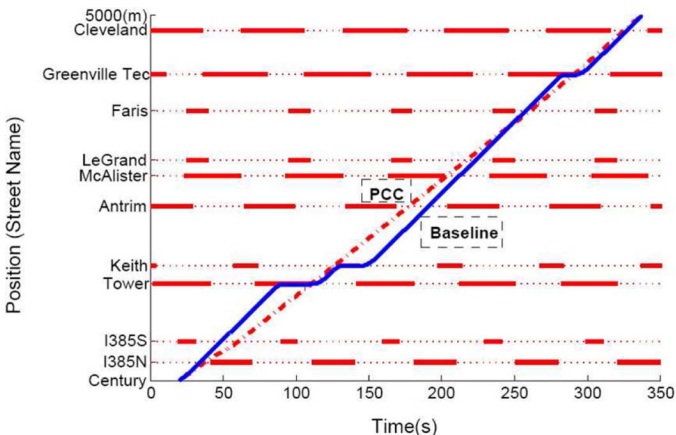


Fig. 9. Second set of PCC and baseline trajectories simulated with Pleasantburg Drive signal timings. Horizontal solid lines represent red intervals.

and the fuel economy gain will reduce to 24% (25.11 m/g versus 20.26 m/g for the baseline).

**B. Multi-Vehicle Scenario**

In this section we investigate the trip time and fuel economy for a fleet of PCC-equipped vehicles in a multi-vehicle simulation. Each vehicle runs a copy of the control strategy presented in Section II in a decentralized fashion. All vehicle and signal parameters are those chosen in Case I of single vehicle scenario.

The former set of constraints in (6) and (7) remains unchanged. When a vehicle is detected at a distance  $\gamma$  in front, the constraint in (8) is also activated with  $x_{target}$  set as the position of the lead vehicle. Otherwise  $x_{target}$  will be the position of the next targeted red light. The parameter  $\gamma$  can be chosen based on a vehicle’s maximum braking distance (See Fig. 10).

Simulations are performed for two fleets of vehicles: A PCC-equipped fleet and a fleet of the same vehicles without PCC. Each fleet has six vehicles aligned initially with the set of initial conditions shown in Table IV.

Figs. 11 and 12 show the trajectories of PCC and baseline fleets for a simulation period of 400 s. The distance traveled by each vehicle as well as the total distance traveled by the vehicles of each fleet during this period are tabulated in Table V for this

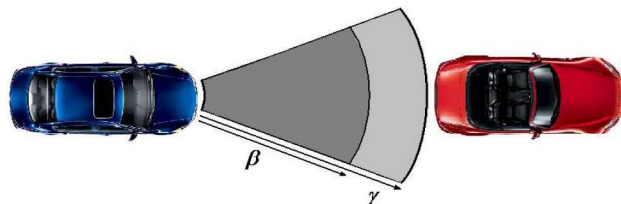


Fig. 10. Illustration of  $\gamma$  as the gap constraint activation area.

TABLE IV  
INITIAL SPEED AND POSITION FOR THE FLEET VEHICLES

| Vehicle | Initial Position(m) | Initial Speed(m/s) |
|---------|---------------------|--------------------|
| 1       | 9000                | 20                 |
| 2       | 8950                | 25                 |
| 3       | 8900                | 20                 |
| 4       | 8800                | 25                 |
| 5       | 8750                | 20                 |
| 6       | 8720                | 15                 |

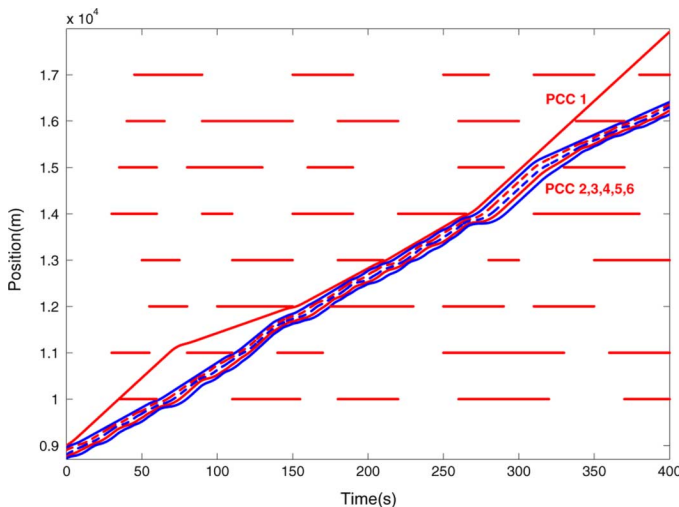


Fig. 11. Trajectories of fleet of PCC vehicles.

simulation case study. The average velocity of the PCC fleet is 19.31 m/s as compared to the 18.53 m/s of the baseline fleet; in other words the PCC fleet is 4.2% faster than the baseline fleet. Fig. 13 shows the gap and gap constraint activation area between each two vehicles in the PCC fleet. It can be seen that the gap always remains above the velocity-dependent gap constraint line.

The vehicle velocity trajectories are fed to PSAT to determine the fuel used by each fleet. The vehicle configuration and parameters are those described in Section III-A. Table VI summarizes the results. The average fuel economy of the PCC fleet is 41.8% better than that of the baseline fleet in this case study.

**IV. CONCLUSION**

Communicating the signal state to vehicles has been recently proposed for improving traffic intersection safety. The positive simulation results of this brief promise that signal-to-vehicle communication technology may also enable reduction of fuel consumption, greenhouse gas emissions, and trip time of future vehicles by predictive velocity planning. In one example case study, predictive use of signal timing reduced fuel consumption by 47% and lowered CO<sub>2</sub> emissions by 56% for simulated

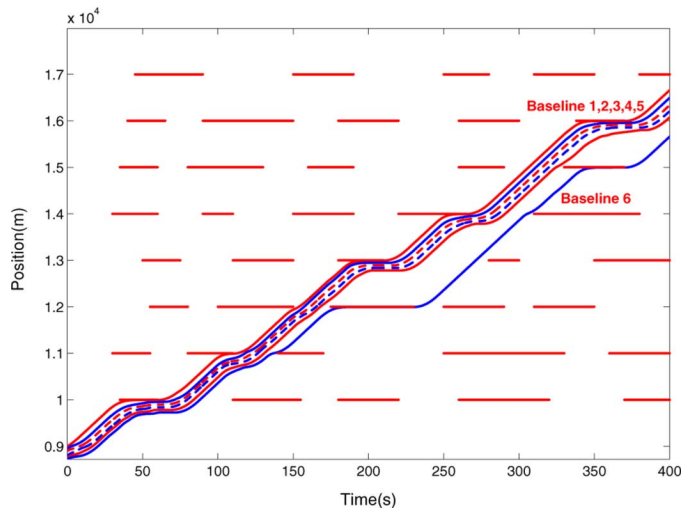


Fig. 12. Trajectories of fleet of Baseline vehicles.

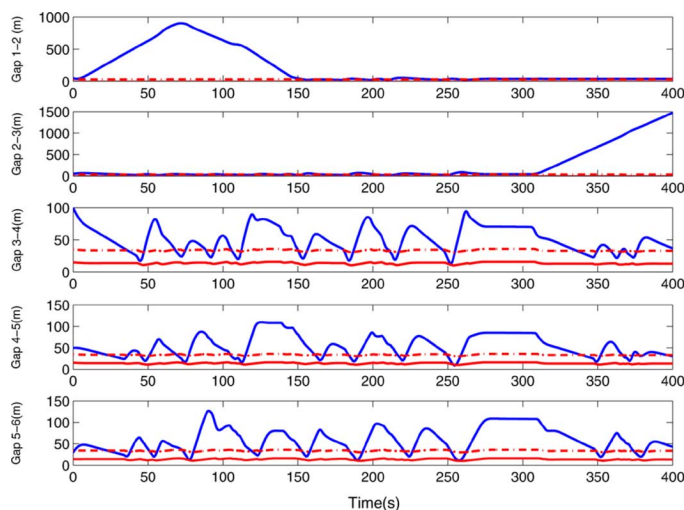


Fig. 13. Gap and Gap constraint between each two vehicles in the PCC fleet. The velocity-dependent constraint line is shown with the lower solid line; the dashed-line shows the border beyond which the constraint is switched on.

TABLE V  
TOTAL TRAVELED DISTANCE FOR PCC AND BASELINE FLEETS

| Vehicle      | 1   | 2   | 3   | 4   | 5   | 6   | Total |
|--------------|-----|-----|-----|-----|-----|-----|-------|
| PCC(km)      | 8.9 | 7.6 | 7.5 | 7.5 | 7.4 | 7.4 | 46.3  |
| Baseline(km) | 7.6 | 7.5 | 7.5 | 7.4 | 7.3 | 7.0 | 44.4  |

TABLE VI  
FUEL ECONOMY COMPARISON FOR PCC AND BASELINE FLEETS

| Vehicle       | 1    | 2    | 3    | 4    | 5    | 6    | Average |
|---------------|------|------|------|------|------|------|---------|
| PCC(mpg)      | 28.7 | 27.7 | 27.9 | 28.1 | 28.1 | 27.5 | 28.0    |
| Baseline(mpg) | 19.2 | 19.7 | 20.2 | 21.3 | 20.3 | 17.3 | 19.7    |

driving through a sequence of 9 traffic lights. Another case study which used real-world traffic signal data showed similar gains. We hope these positive results encourage further research and innovation towards more intelligent traffic intersection control systems. Of course, any gain from the proposed PCC methodology depends on timing and phasing of traffic lights and the distance between them and the vehicle parameters. A detailed

statistical analysis using Monte Carlo simulations is one possible way of determining attainable gains with PCC, and may be a good direction for future simulation analysis.

From an analytical perspective, formulation of the trip optimization in this brief in a model predictive control framework is novel and lends itself well to many traffic-imposed hard constraints. In an ongoing work we hope to evaluate the impact of traffic on the PCC strategy and vice versa by combining a macroscopic traffic model and the microscopic MPC methodology.

#### ACKNOWLEDGMENT

The authors would like to thank Ms. V. Holmes of the Traffic Engineering Department, Greenville, SC, for providing the in-city traffic signal phase and timing information which was used in a simulation case study.

#### REFERENCES

- [1] Texas Transportation Institute, College Station, TX, "Traffic congestion and urban mobility," [Online]. Available: [http://tti.tamu.edu/infofor/media/topics/congestion\\_mobility.htm](http://tti.tamu.edu/infofor/media/topics/congestion_mobility.htm)
- [2] U.S. Department of Transportation, Washington, DC, "The intelligent transportation systems for traffic signal control deployment benefits and lessons learned," 2007. [Online]. Available: [http://www.its.dot.gov/jpdocs/repts\\_te/14321\\_files/a1019-tsc\\_digital\\_n3.pdf](http://www.its.dot.gov/jpdocs/repts_te/14321_files/a1019-tsc_digital_n3.pdf)
- [3] National Transportation Operations Coalition, Washington, DC, "National traffic signal report card," 2007. [Online]. Available: <http://www.ite.org/REPORTCARD/>
- [4] E. Koenders and J. Vreeswijk, "Cooperative infrastructure," in *Proc. IEEE Intel. Veh. Symp.*, 2008, pp. 721–726.
- [5] M. Maile, F. Ahmed-Zaid, L. Caminiti, J. Lundberg, P. Mudalige, and C. Pall, "Cooperative intersection collision avoidance system limited to stop sign and traffic signal violations," NHTSA, Federal Highway Administration, Washington, DC, Tech. Rep. DOT HS 811 048, Oct. 2008.
- [6] U.S. Department of Transportation, Washington, DC, "Video: Demonstration of America's first cooperative vehicle highway system," 2003. [Online]. Available: <http://www.fhwa.dot.gov/ivi/demo1.htm>
- [7] INTERSAFE Project by European Commission Information Society and Media, "INTERSAFE," [Online]. Available: [http://www.prevent-ip.org/en/prevent\\_subprojects/intersection\\_safety/intersafe/](http://www.prevent-ip.org/en/prevent_subprojects/intersection_safety/intersafe/)
- [8] A. Vahidi and A. Eskandarian, "Research advances in intelligent collision avoidance and adaptive cruise control," *IEEE Trans. Intell. Transport. Syst.*, vol. 4, no. 3, pp. 143–153, Mar. 2003.
- [9] E. Brockfeld, R. Barlovic, A. Schadschneider, and M. Schreckenberg, "Optimizing traffic lights in a cellular automaton model for city traffic," *Phys. Rev. E*, vol. 64, no. 5, p. 056132, Oct. 2001.
- [10] D.-W. Huang and W.-N. Huang, "Traffic signal synchronization," *Phys. Rev. E*, vol. 67, no. 5, p. 056124, 2003.
- [11] C. Gershenson, "Self-organizing traffic lights," *Complex Syst.*, vol. 16, no. 1, pp. 29–53, 2005.
- [12] K. Dresner and P. Stone, "A multiagent approach to autonomous intersection management," *J. Artificial Intell. Res.*, vol. 31, pp. 591–656, 2008.
- [13] M. VanMiddlesworth, K. Dresner, and P. Stone, "Replacing the stop sign: unmanaged intersection control for autonomous vehicles," in *Proc. 5th Workshop Agents Traffic Transport. Multiagent Syst.*, Estroil, Portugal, May 2008, pp. 94–101.
- [14] U.S. Department of Transportation, Washington, DC, "Urban drive control," 1999. [Online]. Available: <http://www.itsbenefits.its.dot.gov/its/benecost.nsf/ID/876D690DAB8FCA6B8525733A006D5BCC?OpenDocument&Query=BAApp>
- [15] R. Sengupta, S. Rezaei, S. Shladover, D. Cody, S. Dickey, and H. Krishnan, "Cooperative collision warning systems: Concept definition and experimental implementation," *J. Intell. Transport. Syst.: Technol., Plan., Operat.*, vol. 11, no. 3, pp. 143–155, 2007.
- [16] C.-Y. Chan and B. Bougler, "Evaluation of cooperative roadside and vehicle-based data collection for assessing intersection conflicts," in *Proc. IEEE Intel. Veh. Symp.*, 2005, pp. 165–170.



- [17] K. Nagel, P. Wagner, and R. Woesler, "Still flowing: Approaches to traffic flow and traffic jam modeling," *Oper. Res.*, vol. 51, no. 5, pp. 681–710, 2003.
- [18] K. Nagel, "Particle hopping models and traffic flow theory," *Phys. Rev. E.*, vol. 53, no. 5, p. 4655, 1996.
- [19] S. P. Hoogendoorn and P. H. L. Bovy, "State-of-the-art of vehicular traffic flow modelling," *Proc. Inst. Mechan. Eng., Part I: J.Syst. Control Eng.*, vol. 215, no. 4, pp. 283–303, 2001.
- [20] T. D. Gillespie, "Fundamentals of vehicle dynamics," SAE Int., Warrendale, PA, 1992.
- [21] J. M. Maciejowski, *Predictive Control with Constraints*. Englewood Cliffs, NJ: Prentice-Hall, 2002.
- [22] M. M. Seron, G. C. Goodwin, and J. A. Dona, *Constrained Control and Estimation*. New York: Springer, 2005.
- [23] A. Bemporad, "Model predictive control design: New trends and tools," in *Proc. IEEE Conf. Dec. Control*, 2006, pp. 6678–6683.
- [24] Argonne National Laboratory, Argonne, IL, "Powertrain system analysis toolkit," 2007. [Online]. Available: <http://www.transportation.anl.gov/software/PSAT/index.html>